

FIG. 8. Density of states contribution and energy surfaces associated with critical points in the $E(\mathbf{k})$ spectrum.

points¹⁶ will occur when $\nabla(E(\mathbf{k}))=0$. Thus, the critical points in k space will be found where the energy bands are very flat. Since $E(\mathbf{k})$ is a continuous function, we may expand the energy about the critical energy $E_c(\mathbf{k})$ as a Taylor series, where the linear terms are zero since $\nabla(E(\mathbf{k}))=0$. Thus, we have

$$E(\mathbf{k}) = E_c(\mathbf{k}) + \alpha_1 q_1^2 + \alpha_2 q_2^2 + \alpha_3 q_3^2 + \dots, \quad (1)$$

where $\mathbf{q} = \mathbf{k} - \mathbf{k}_c$ and $\alpha_i = \partial^2 E(\mathbf{k}) / \partial k_i^2$.

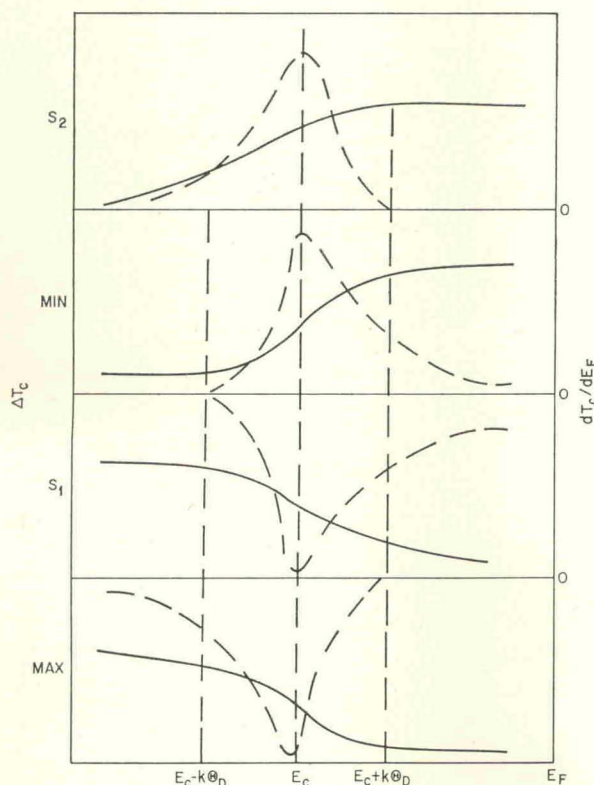


FIG. 9. Energy dependences of ΔT_c (solid line) and $\partial \Delta T_c / \partial E_F$ (broken line) as E_F passes through a critical point in the $E(\mathbf{k})$ spectrum. S_1 , S_2 , min., and max. refer to the critical points illustrated in Fig. 8.

¹⁶ J. M. Ziman, *Principles of the Theory of Solids* (Cambridge University Press, New York, 1964), p. 48.

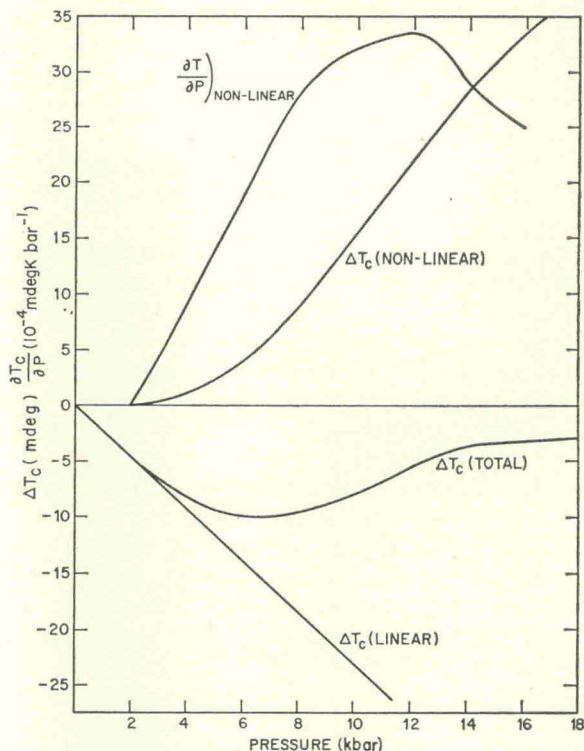


FIG. 10. Breakdown for Re of ΔT_c as a function of pressure into its linear and nonlinear contributions.

If, for example, all the α_i were positive, then there would be a local minimum in $E(\mathbf{k})$, and the additional contribution to the density of states would be

$$\Delta N(E) = 0, \quad E < E_c, \\ \propto (E - E_c)^{1/2}, \quad E > E_c. \quad (2)$$

The energy dependence of $\Delta N(E)$ for this and the other three possible types of critical points is shown in Fig. 8, where S_1 and S_2 denote saddle points of indices 1 and 2. The shapes of the constant energy surfaces represented by Eq. (1) with all possible combinations of signs for α_i are also shown. Thus, as the energy passes through the critical energy corresponding to a local minimum in $E(\mathbf{k})$, a new surface is formed; or, conversely, on passing through a local maxima, a surface is destroyed. A transition through a saddle point results in the formation (or disruption) of a "neck," i.e., the transition from an open to a closed section of Fermi surface (or vice versa).

In the nearly free-electron approximation of a metal with pressure-independent potentials, the topology of the Fermi surface remains unchanged under an isotropic compression, but changes may occur if there is distortion. However, calculations based on the pseudopotential approximation to the nearly free-electron model show that the form factor depends upon volume and thus the connectivity of the Fermi surface at boundary points can change under isotropic compression.

sion.¹⁷ In metals containing non-*s* electrons, flat regions in $E(k)$ curves may also occur at k values other than boundary points. If these regions are associated with strong hybridization, then changes in the lattice parameter can produce significant energy shifts relative to the Fermi energy. Thus, when these regions lie close to the Fermi surface, abrupt changes in topology can occur.

The first systematic study of the effects of such abrupt changes in topology on the thermodynamic and kinetic properties of a metal was undertaken by Lifshitz.¹⁵ Markarov and Bar'yakhtar⁴ extended this study to include the effects on the superconducting properties by introducing the change in the density of states into the energy-gap equation of the Borden-Cooper-Schrieffer (BCS) model.¹⁸ They investigated the behavior of T_c and $\partial T_c/\partial E_F$ as functions of E_F (the Fermi energy) at energies close to E_c ; their results are summarized in Fig. 9. Over the energy range $(E_c - k\Theta_D) \leq E_F \leq (E_c + k\Theta_D)$, where Θ_D is the Debye temperature, T_c increases sharply at the critical points corresponding to S_2 or a minimum, whereas T_c decreases sharply at S_1 or a maximum. In all cases, $\partial T_c/\partial E_F$ exhibits an extremum at $E_F = E_c$. From an experimental point of view, we are concerned with $\partial T_c/\partial P$, but since we may consider $\partial T_c/\partial P = (\partial T_c/\partial E_F)(\partial E_F/\partial P)$ and since we may reasonably assume that $\partial E_F/\partial P$ will vary slowly with pressure, any rapid variation of $\partial T_c/\partial E_F$ will also appear as a rapid variation of $\partial T_c/\partial P$.

In Fig. 10, we demonstrate the breakdown of ΔT_c for Re into its linear and nonlinear components. The variation of $(\partial T_c/\partial P)_{\text{nonlinear}}$ as a function of pressure, derived from $\Delta T_c(\text{nonlinear})$ is also plotted. The similarity between the pressure dependence of ΔT_c and $\partial T_c/\partial P$ for the nonlinear contribution and the energy dependence curves at the points S_2 and minimum shown in Fig. 9 is evident. Similar plots were made for the Re-Os alloys containing less than 0.2-at.% Os and, in particular, we show the plot for the 0.11-at.% Os in Fig. 11.

In the case of pure Re, the nonlinear contribution was estimated to start at pressures above ~ 2 kbar and a maximum occurs in $(\partial T_c/\partial P)_{\text{nonlinear}}$ at a pressure $P_c \sim 12$ kbar. On alloying with osmium, the pressure at which the nonlinear contribution commences rapidly falls to zero, as shown for example, by the curve for the addition of 0.11-at.% Os. In addition, it is found that the curve for $(\partial T_c/\partial P)_{\text{nonlinear}}$ does not fall smoothly above P_c , but has a step approximately 6 kbar wide. This behavior was not observed for pure Re, but this may well be due to the limitations of our pressure range. This form of the curve for the Os alloys suggests the possibility that more than one critical

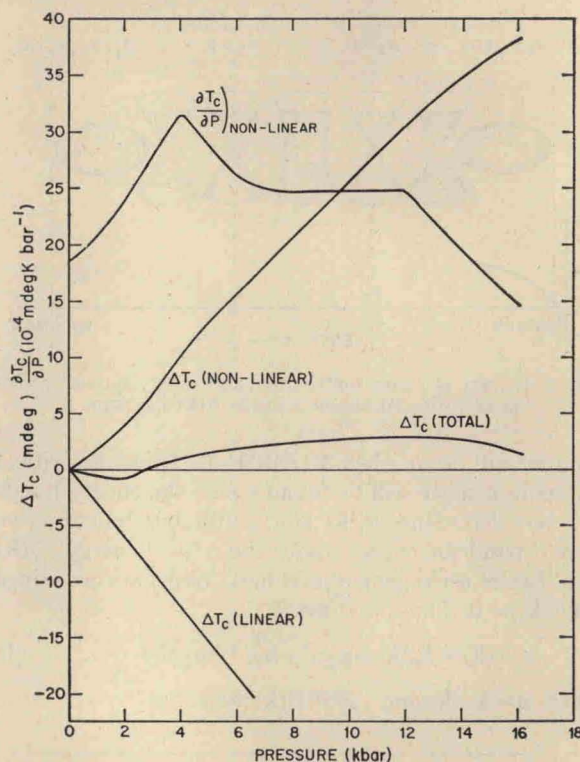


FIG. 11. Breakdown for Re 0.11-at.% Os of ΔT_c as a function of pressure into its linear and nonlinear contributions.

point may be involved. Furthermore, P_c decreases roughly linearly with the addition of Os and goes to zero at the critical composition ~ 0.14 at.% (see Fig. 12). It is evident from Figs. 6 and 7 that P_c increases with concentration in the Re-W and Re-Mo systems, but, unfortunately, our pressure range was insufficient to reach P_c for these systems.

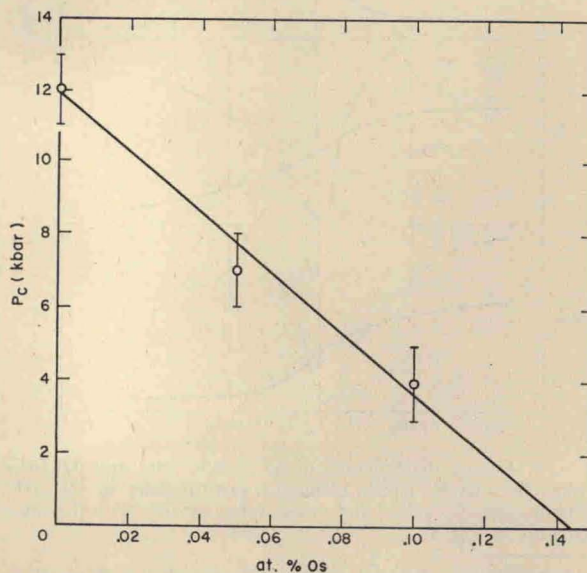


FIG. 12. Variation of P_c with Os concentration.

¹⁷ W. A. Harrison, *Physics of Solids at High Pressure* (Academic Press Inc., New York, 1965), p. 3; L. M. Falicov, *ibid.* p. 30.

¹⁸ J. Bardeen, L. Cooper, and J. Schrieffer, *Phys. Rev.* **108**, 1175 (1957).